# Predissociation of the $A^2\Sigma^+$ ($v'$=4) States of OH: Effects of Multichannel Asymptotic Interactions

**Sungyul Lee**

*Department of Chemistry, Kyunghee University, Kyungki-do 449-701, Korea*
*Received March 7, 2000*

Quantum mechanical analysis is presented for the photodissociation dynamics of the $v'$=4 levels of the $A^2\Sigma^+$ state of the OH molecule. We focus on the effects of the multichannel interactions between the asymptotically degenerate states in the recoupling region to see how they affect the dynamics near the predissociating resonances. Both the scalar (total cross section and branching ratios) and the vector properties (angular distributions and alignment parameters) of O($^3P_j$, $j$ = 0, 1, 2) are treated. The resonances are predicted to be highly Lorentzian, and the branching ratios do not change much across them. Vector properties, however, show very delicate effects of the multichannel interactions and overlapping near the isolated and overlapping resonances. Computed resonance lifetimes agree reasonably well with experimental results.

## Introduction

Diatomic photodissociation to open-shell atoms has received considerable attention recently, because invaluable information on the electronic states and the non-Born-Oppenheimer interactions could be obtained by theoretical and experimental studies on the process. Freed and co-workers[1] were the first to treat this interesting case theoretically. They showed that, when the molecule dissociates to open-shell atoms, there may be more than one repulsive states involved in the dynamics, and that the interactions between the asymptotically degenerate states can give profound effects on the properties of the photofragments. This is due to the fact that at large internuclear distances the separations between the electronic states become comparable to the magnitude of the interactions, and that extensive redistribution of quantum flux may occur. The effects of these multichannel asymptotic interactions were treated in photodissociation of diatomic molecules such as $CH^+$ [Ref. 2], $Na_2$ [Ref. 3], NaH [Ref. 4], and hydrogen halides such as HCl [Ref. 5-7] and HBr [Ref. 8, 9]. In these situations, the dissociation is direct, and the electronic states dissociate to a single atomic term.

In contrast, the *predissociation* of the OH molecule is a much more complicated process. The electronic states involved in the dynamics correlate with two atomic terms (O($^3$P) and O($^1$D): see Figure 1). Several different kinds of interactions may affect different properties of photofragments at different internuclear distances. First, spin-orbit couplings between the bound $A^2\Sigma^+$ and the repulsive $^4\Sigma^-$, $^2\Sigma^-$ and $^4\Pi$ states in Franck-Condon region mainly accounts for the total cross sections and the widths (lifetimes) of the predissociating resonances. Second, multichannel interactions between the asympotically degenerate $X^2\Pi$, $^4\Sigma^-$, $^2\Sigma^-$ and $^4\Pi$ states in the asymptotic region may also give important effects on the branching ratios and the vector properties of O($^3P_j$, $j$ = 0, 1, 2). Finally, quantum interference between the direct (*via* $^2\Sigma^-$) and the indirect (predissociating *via* $A^2\Sigma^+$ through the repulsive $^4\Sigma^-$, $^2\Sigma^-$ and $^4\Pi$ states) pathways were predicted[8-11] to give novel features of asymmetric resonances and strongly changing properties of photoproducts near the resonances.

More interestingly, the relative importance of these effects also highly depends on the vibrational quantum number $v'$ of the $A^2\Sigma^+$ state. For low-lying $v'$ = 2 and $v'$ = 3 levels, the predissociation occurs predominantly through the single repulsive state, $^4\Sigma^-$. The Franck-Condon factor for transitions from the ground $X^2\Pi$ state to the repulsive $^2\Sigma^-$ state is very small, and the effects of the quantum interference are minimal. Therefore, the dynamics looks like normal predissociation, in the sense that the resonance is Lorentzian, and that the branching ratios and the vector properties of the photofragments change very little across the resonance.[10] For the higher vibrational levels with $v' \geq 7$, the effects of the multichannel asymptotic interactions and those of the quantum interference coexist, and dynamics of predissociation near the resonances is very intriguing.[10-13] Although it will be very interesting to study the separate effects of these two different kinds of phenomena, it would only be possible theoretically by simulating the dynamics employing the *vanishing* $X^2\Pi$-$^2\Sigma^-$ transition dipole moment. This situation is, of course, unattainable in experiments.

The $v'$ = 4 levels are at the borderline of these two cases. The $^2\Sigma^-$-$X^2\Pi$ transition dipole moment is still very small near the $v'$ = 4 resonances, and so the effects of quantum interference may be negligible. On the other hand, since more than one repulsive excited states ($^4\Sigma^-$, $^2\Sigma^-$ and $^4\Pi$) are involved for dissociation near the $v'$ = 4 resonances, the interactions among these asymptotically degenerate repulsive states in the recoupling region may affect the fragment properties significantly. Therefore, the $v'$ = 4 resonances may give excellent situation where the *isloated* effects of multichannel asymptotic interactions on the predissociation can be seen and may be verifiable by experiments.

Although the dynamics of the OH molecule proves very interesting, only the lifetimes (widths)[14-19] of the lower resonances of the $A^2\Sigma^+$ state had been of interest for a long time. Recently, however, the resonance profiles, the branching ratios and the vector properties of the oxygen atom produced from the predissociation were also studied, notably by Par-

lant and Yarkony.[20] It was found that the behavior of the product properties near the resonances may indeed be extremely interesting. Although preliminary approximate treatments[21] of the OH predissociation processes found that the branching ratios of O($^3P_j$, $j = 0, 1, 2$) could provide detailed information on the dissociation pathways, no systematic analysis was made on the vector properties.

In this work, we analyze the effects of the multichannel asymptotic interactions on the properties of the triplet oxygen atom produced from OH photodissociation near the $v' = 4$ predissociating resonances. We employ full quantal theory which is the genaralization of Freed and co-workers',[1] treating the situation where more than one atomic term is involved in the dynamics. All the spin-orbit and rotational couplings are included, except the hyperfine interactions. No assumptions need to be made for Hund's coupling cases for the electronic states. We treat the resonance lifetimes (widths), resonance profiles, branching ratios of O($^3P_j$, $j = 0, 1, 2$), and the vector properties such as the angular distributions and the fluorescence anisotropy parameters. We find that the small $^2\Sigma^-$-$X^2\Pi$ Franck-Condon factors result in highly Lorentzian resonances for $v' = 4$, and therefore, that the branching ratios of O($^3P_j$, $j = 0, 1, 2$) remain constant across the resonances, showing that the effects of the quantum interference are minimal. We find, however, that the influence of the multichannel interactions in the asymptotic region affects the dynamics significantly. The vector properties exhibit slow and monotonic changes near the isolated resonances as the consequence of this latter effect. The overlapping resonances are affected as well. The $F_1$ and $F_2$ components, with the same nuclear rotational quantum number $N'(=J \pm S)$ but with different total angular momentum quantum numbers $J$, ($F_1$ represents $N' = J-1/2$, while $N' = J+1/2$ for $F_2$) perfectly overlap in integral cross sections, indicating that their separations are much smaller than their widths. The vector properties, however, show noticeable structures near the $F_1$ and $F_2$ resonances. Computed lifetimes of the $v' = 4$ resonances compare well with experimental values.

## Theory and Computational Methods

The theory employed here is the generalization of Freed and co-workers [Ref. 1]. It can treat the very general situations where there can be more than one atomic term involved in the dynamic process, and where there can be all kinds of crossings (and avoided crossings) between potential curves. The theory was described in detail in [Ref. 10], and it is only briefly summarized here. The most important ingredient of the theory is the frame transformation matrices that connect the adabatic Born-Oppenheimer (ABO) states to the corresponding atomic terms. Since there occur explicit curve crossings in the Franck-Condon region between the $A^2\Sigma^+$ state and the repulsive $^4\Sigma^-$, $^2\Sigma^-$ and $^4\Pi$ states in OH predissociation process, and since two oxygen terms ($^3P$ and $^1D$) are involved in the dissociation process, *two* transformation matrices are constructed, each of which describes the correlation between the ABO states and the corresponding atomic term.

Two basis sets are employed to describe the dissociation dynamics in the molecular and asymptotic region, respectively. The first basis (ABO basis) $|C\Lambda S\Sigma p>_J$ is a body-fixed basis derived from Hund's coupling cases. Hund's case (a) basis is used here, although other coupling cases may also be employed as long as all the interactions are included to evaluate the total Hamiltonian. In this basis, the quantum numbers $\Lambda$, $S$, $\Sigma$ possess their usual meanings, $C$ represents the correlating atomic term, and $p$ is the parity. The electronic Hamiltonian is evaluated using this ABO basis. The second basis set $|JM_j l j_O j_H>$, which is called 'asymptotic' molecular basis, diagonalizes the total Hamiltonian at infinite internuclear distances. This basis is employed to properly describe the transition amplitudes for dissociation to each atomic fine structure state of the atomic fragments with total electronic angular momentum quantum numbers $j_O$ and $j_H$. $j = j_O+j_H$, and $J(=j+l)$ is the total final angular momentum quantum number. $M$ is the space-fixed component of $J$. Since the spin-orbit Hamiltonian and the rotational part of the kinetic energy term are diagonal in this basis at large internuclear distances, they are evaluated by employing the asymptotic basis. These two basis sets are related to each other by the $r$-independent transformation matrix $<jlj_Oj_H|C\Lambda S\Sigma p>_J$. The off-diagonal elements of the rotational term, when transformed to ABO basis, represent Coriolis couplings.

The vibrational wave functions of the ground state are obtained by employing the Cooleys procedure,[22] and the scattering wave function is propagated by the Renormalized Numerov method.[23] Appropriate boundary conditions are imposed at the end of the propagation (at 25 a.u.), and the convergence was checked by increasing the number of integration steps to 3000. The photodissociation amplitudes are computed by employing the Golden rule. The potential curves, transition dipole moments and the spin-orbit couplings employed in the present calculation were described in [Ref. 10] in detail. The branching ratios of the three lowest fine structure states of the oxygen atom ($^3P_j$, $j = 0, 1, 2$) are defined as the ratios of the partial cross sections for production of these two states to the total cross section. Two vector properties[24-27] are considered in the present work. The anisotropy parameters ($\beta_D$) of the angular distribution of O($^3P_j$, $j = 0, 1, 2$) are those usually employed to describe the angular distributions, as defined by the familiar expression for the differential cross section,

$$\frac{d\sigma}{d\Omega_{\hat{k}}} \propto \{1 + \beta_D P_2(\hat{k} \cdot \hat{z})\} \tag{1}$$

The alignment parameter ($\beta_S$) is a measure of the distribution of the magnetic sublevels, and is related to the familiar polarization ratio $P$ by

$$P \equiv \frac{I_{//} + I_{\perp}}{I_{//} + I_{\perp}} = \frac{3\beta_s}{4 + \beta_s}$$

The explicit expressions for the integral cross sections, $\beta_D$ and $\beta_S$ were given by Freed and co-workers.[1] The $\beta_D$ parameter can be expressed as

$$\beta_D = \frac{\sigma_{00;20}}{\sigma_{00;20}}, \quad (3)$$

where the denominator is proportional to the total cross section, and the numerator is a coherent sum of the contributions from three $J$'s ($J = J_i, J_i \pm 1$),

$$\sigma_{00;20} = \frac{\sum_{J_F J_F} \alpha_{J_F} \alpha_{J_F}}{\sum_{J_F} \alpha_{J_F}}. \quad (4)$$

The $\alpha$'s in Eq. (4) are products of the geometrical and dynamic factors (see Ref. 1).

It must be noted that the $A^2\Sigma^+$ state is approximately Hunds case (b). This is realized naturally in our method (in contrast to our previous approximate treatments[21]) without assuming the Hund's case for this state, resulting from the combination of the employed Hund's case (a) basis by the couplings included in the theory. The location of the resonances corresponding to the rovibrational levels of the $A^2\Sigma^+$ state is computed to depend on $N'(N'+1)$ ($N' = J \pm S$), which is characteristic of Hund's case (b). Thus, the wave function of the $A^2\Sigma^+$ state is also characterized by the nuclear quantum number $N'$, giving different dynamics to the $F_1$ and $F_2$ components (with identical $N'$ but different $J$) *via* the transition amplitudes to be employed for the evaluation of vector properties in Eqs. (1) and (2).[1]

## Results

The potential curves of the electronic states included in the present calculations are depicted in Figure 1. The $X^2\Pi$, $^4\Sigma^-$, $^2\Sigma^-$ and $^4\Pi$ states correlate with O($^3$P), while the $A^2\Sigma^+$, $^2\Delta$ and $2^2\Pi$ states correlate with O($^1$D). The zero of energy is defined in this paper as the statistical average of the energies of O($^3P_j$, $j = 0, 1, 2$). The dynamics of photodissociation is affected both by the spin-orbit interactions in the Franck-Condon region between the crossing, $A^2\Sigma^+$, $^4\Sigma^-$, $^2\Sigma^-$ and $^4\Pi$ states, and by the nonadiabatic (spin-orbit and Coriolis) interactions in the asymptotic region between the asymptotically degenerate states correlating with the O($^3$P) term.

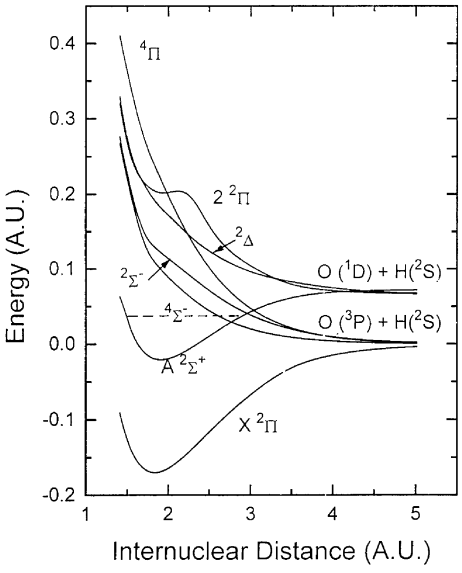


**Figure 1**. Potential curves of OH. The zero of energy is defined as the statistical average of the energies of O($^3P_j$, $j = 0, 1, 2$). The dotted line represents the $v' = 4$ and $N' = 0$ level of the $A^2\Sigma^+$ state.

There are two important factors that may affect the dynamics of predissociation near the $v' = 4$ resonances. First, quantum interference between the direct (by the $^2\Sigma^-$-$X^2\Pi$ transition) and the indirect (*via* the $A^2\Sigma^+$ state) dissociation pathways may influence the dynamics, as we showed in a number of occasions. Second, the asymptotic interactions among the repulsive states at large internuclear distances may also give interesting effects on the scalar and vector properties. Figure 2 presents the total cross section and the partial cross sections for producing the fine structure states of the triplet oxygen atom, O($^3P_j$, $j = 0, 1, 2$) near the ($N' = 14$, $J = 14.5$, $v' = 4$) level of the $A^2\Sigma^+$ state, excited from the $J_i = 15.5$ and $v_i = 0$ level of the $X^2\Pi_{3/2}$ state. The resonance is highly Lorentzian, and the branching ratios for production of O($^3P_j$, $j = 0, 1, 2$) are essentially constant (0.07, 0.36, 0.57 for O($^3P_j$, $j = 0, 1, 2$), respectively) as functions of the energy near the resonance, which is characteristic of the Lorentzian resonances. Therefore, the effects of the quantum interference, which gave asymmetric resonances and rapidly-changing fragment properties for $v' \geq 7$ resonances, are minimal here. This observation is also verified by the fact that essentially identical results were obtained when the $^2\Sigma^-$-$X^2\Pi$ transition moment is put to vanish, thus eliminating the interference from the direct dissociation pathway.

The influence of the multichannel interactions between the electronic states correlating with O($^3$P) at large internuclear distances on the photodissociation process may be elucidated in a number of ways, but the most direct way is to examine the effects on the vector properties, since the scalar properties may somewhat be insensitive. As we discussed in [Ref. 12], the vector properties remain constant near the Lorentzian resonances only if they are isolated and the dissociation is through a single dissociative state. Figure 3 shows the $\beta_D$ parameters representing the angular distributions of

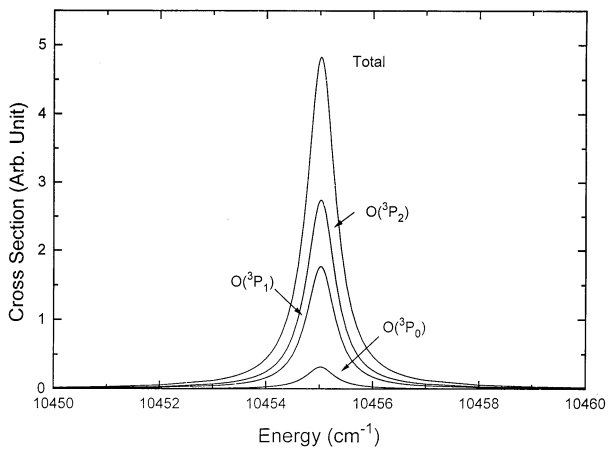


**Figure 2**. The cross sections near the isolated resonance ($N' = 14$, $J = 14.5$, $v' = 4$).

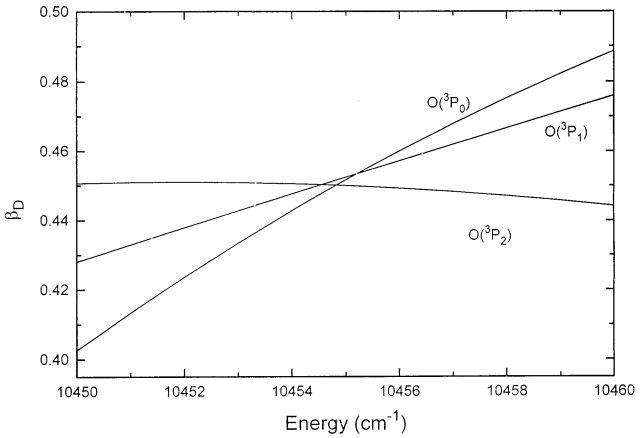


**Figure 3**. The $\beta_D$ parameters near the isolated resonance in Figure 2.

$O(^3P_j, j = 0, 1, 2)$ near the same *isolated* resonance shown in Figure 2. In contrast to the branching ratios, the $\beta_D$ parameters show monotonic but noticeable changes across the isolated resonance. Figure 4 also shows similar behavior of the $\beta_S$ parameter. This is the indication of the multichannel asymptotic couplings among the repulsive states correlating with $O(^3P)$, as we discussed in previous simulation for the isolated $v' \geq 7$ resonances: When the $X^2\Pi$-$^2\Sigma^-$ transition dipole moment (consequently, the effects of quantum interference) and the interactions between the asymptotically degenerate $X^2\Pi$, $^4\Sigma^-$, $^2\Sigma^-$ and $^4\Pi$ states were arbitrarily eliminated, the vector properties changed very little across the resonance, showing that the monotonic changes of the vector properties are the results of the multichannel asymptotic interactions between the repulsive states. In the present case of the $v' = 4$ resonance, the isolated effects of the multichannel interactions on the vector properties $\beta_D$ and $\beta_S$ are clearly seen in Figure 3 and 4, and therefore these effects may be verified experimentally. It should be stressed that these effects are distinct from those of the quantum interference, since the latter would give much more drastic changes in the vector properties near the resonance, as discussed in [Ref. 12].

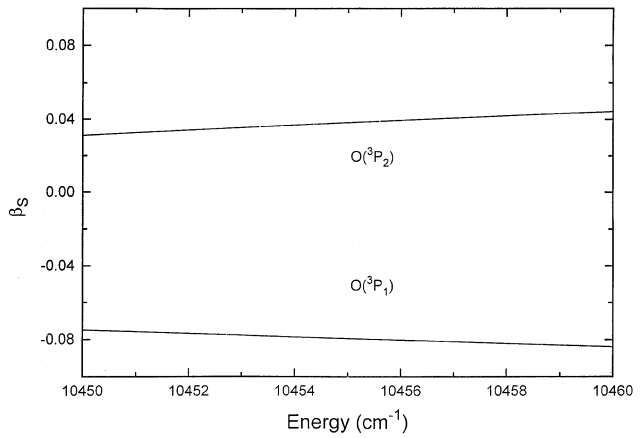


**Figure 4**. The $\beta_S$ parameter near the isolated resonance in Figure 2.

The resonance in Figure 2 is an isolated one, since the other resonances ($J = 15.5$ and 16.5, $v' = 4$) accessible from the $J_i = 15.5$ level of the $X^2\Pi_{3/2}$ state are of $N' = 15$, and they are separated from the $N'$=14 level by about 500 $cm^{-1}$. These two resonances are the $F_1$ and $F_2$ components of the $N' = 15$ level. For the lower vibrational levels, $v' = 2$ and 3, of the $A^2\Sigma^+$ state, the separation of these two components is about 10 times as large as their widths, and thus they appear separated, as we showed in [Ref. 10]. Since the widths of the $v' = 4$ resonances are larger, it will be very interesting to see if the $F_1$ and $F_2$ components of these higher-lying resonances are separated or overlapping. Figure 5 shows the $F_1$ and $F_2$ components of the ($N' = 2$, $v' = 4$) level, optically accessible from the $J_i = 1.5$ level of the $X^2\Pi_{3/2}$ state. The two components are perfectly overlapping, and the branching ratios do not change across the resonances, lacking signature for the overlapping. This indicates that the splitting of the $v' = 4$ resonances, attributed to different couplings of $F_1$ and $F_2$ components to the $^2\Pi$ states, is much smaller than their widths. The vector properties, however, show very interesting behavior near the overlapping resonances. Figure 6 depicts the $\beta_D$ parameters near the $F_1$ and $F_2$ resonances, and it can be seen that all of the $\beta_D$ parameters exhibit noticeable structures, clearly showing the effects of the overlapping. The behavior of the $\beta_S$ parameter is similar but weaker. It will be interesting to compare these latter findings with the behavior of the vector properties near the neighboring (Lorentzian) $F_1$ and $F_2$ resonances with $v' = 2$, $N' = 4$ treated elsewhere.[13] Since the separation between the two components of the $v' = 2$ resonance is much larger than their widths, the two Lorentzian resonances do not overlap. Therefore, only the term with specific value of $J$ is important in the sum in the expression of $\beta_D$ parameters (see Eqs. (3) and (4) above) near the resonance corresponding to $J$. Near the $F_1$ or $F_2$ resonance, the values of $\beta_D$ will be different, and the $\beta_D$ parameters exhibit rapid changes across these neighboring Lorentzian ($v' = 2$, $N' = 4$) resonances. In the present case of overlapping $v' = 4$ resonances in Figure 5, however, the vector properties $\beta_D$ do not change much but shows somewhat

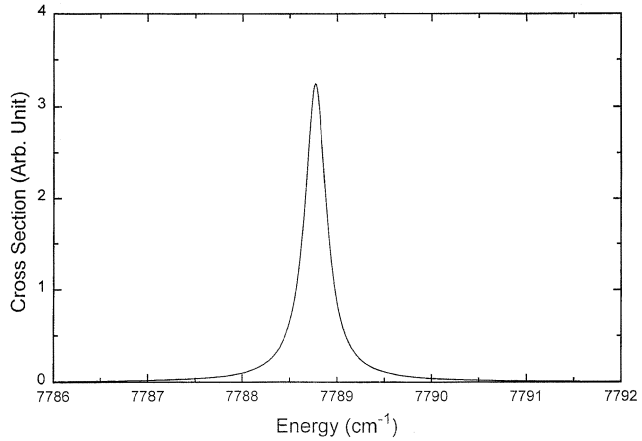


**Figure 5**. The perfectly overlapping $F_1$ and $F_2$ resonances (with $J_f$=3/2, and $J_f$=5/2, respectively) of the $N' = 2$ and $v' = 4$ level of the $A^2\Sigma^+$ state.

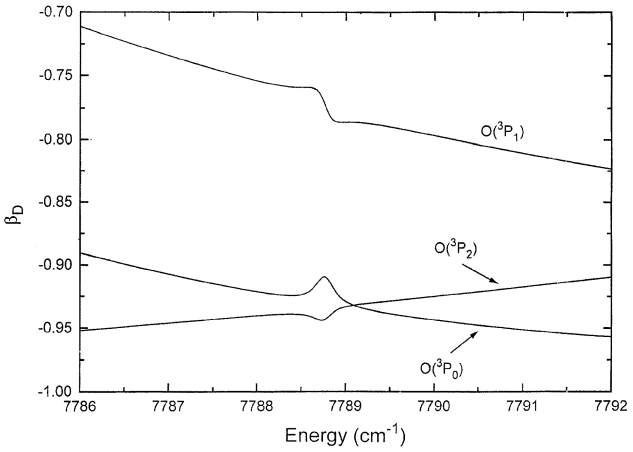


**Figure 6**. The $\beta_D$ parameters near the overlapping resonances ir Figure 5.

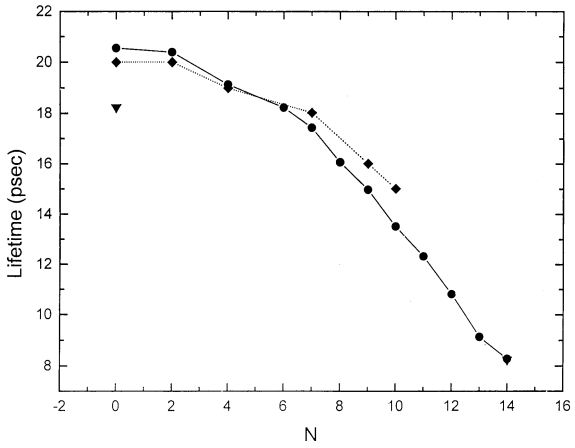


**Figure 7**. The lifetimes of the $v' = 4$ resonances. Circles: present results; Diamonds: experimental results (Ref. 16); Inverse triangles ($N' = 0$ and $N' = 14$): computed results by Parlant and Yarkony (Ref. 20).

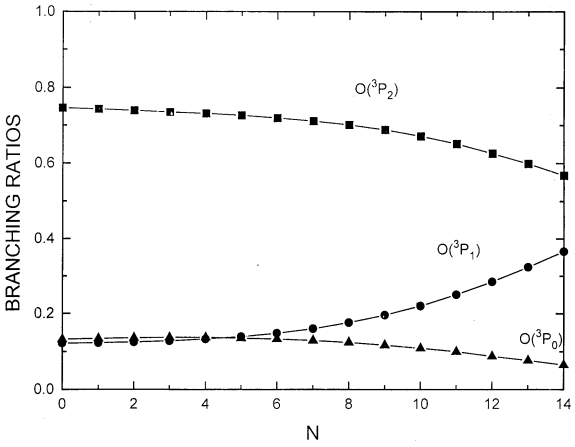


**Figure 8**. The branching ratios of $O(^3P_j, j = 0, 1, 2)$ as functions of $N'$. The branching ratios were computed from the partial cross sections at the peak of the resonance.

"averaged" behavior along with the signature of overlapping not seen in the branching ratios. This finding is in agreement with the fact that the vector properties are more sensitive to details of the dynamics than the scalar properties.[1,2]

The widths (lifetimes) of the predissociating resonances of OH were of much interest in many investigations,[14-19] since the widths are related to the magnitudes of bound - continuum couplings. Most of the theoretical and experimental works were focused on the $v' = 2$ and $v' = 3$ resonances, but there exists fragmentary information on the $v' = 4$ resonances as well. Figure 7 gives the computed lifetimes of the$F_1$ components of the $v' = 4$ resonances, and comparison is also made with the experimental observations.[16] The lifetimes decrease with $N'$, indicating that the probability of predissociation increases with $N'$. The agreement is generally good, typical error being about 10% for higher $N'$. We also computed the lifetimes of the $F_2$ components, and find that they are very similar to those of the $F_1$ components. Our computed lifetime for $N' = 0$ resonance is about 10% larger than that given by Parlant and Yarkony,[20] but the lifetime for $N' = 14$ resonance agrees very well with their results.

Figure 8 depicts the branching ratios of $O(^3P_j, j = 0, 1, 2)$ as functions of $N'$. Since there exist no measured branching ratios of $O(^3P_j, j = 0, 1, 2)$ produced from the predissociation of the $A^2\Sigma^+$ state, it is impossible to compare the computed branching ratios with experimental observations. Thus, we compare our computed branching ratios (Figure 8) with the recent theoretical work by Parlant and Yarkony.[20] For $N' = 14$ and $v' = 4$ resonance ($F_1$ component), our computed branching ratios (0.07, 0.36, 0.57) of $O(^3P_j, j = 0, 1, 2)$, are similar to those given by Parlant and Yarkony[20]: (0.12, 0.28 and 0.60). On the other hand, the branching ratios (0.14, 0.13, 0.74) for $N' = 0$ and $v' = 4$ resonance are a bit different from those computed by Parlant and Yarkony. They predicted that almost no $O(^3P_0)$ would be produced at $N' = 0$ resonance, while the ratios for $O(^3P_j, j = 1, 2)$ were given as about 0.1 and 0.9, respectively. This slight disagreement may probably due to the differences in the*ab initio* data employed here and in Parlant and Yarkonys work. Although the qualitative predictions made in the present analysis do not depend much on the detailed topology of the potential curves and the interactions thereof, the numerical values of the fragment properties are known to be rather sensitive to this information, especially for low energy (low $N'$ for given $v'$). Therefore, systematic variation of the *ab initio* potential curves and the interactions would have to be made in order to compare quantitatively with the experimental results.

The branching ratios[5,20,28-30] may give invaluable information on the dissociation pathway, because each of the dissociative states possesses characteristic branching ratios, and deviations from the single-state branching ratios indicate dissociation through more than one state. For $N' = 0$, the ratios are (0.134, 0.123, 0.746), which are different from any of the branching ratios resulting from the single-state dissociation through the $^4\Sigma^-$, $^2\Sigma^-$ or the $^4\Pi$ states: (0.222, 0.167, 0.611), (0.111, 0.333, 0.556) and (0.444, 0.250, 0.306), respectively.[20] Thus, it seems that the predissociation near $N' = 0$ results from the combination of more than one repulsive state, presumably through the $^4\Sigma^-$ and the $^2\Sigma^-$ states. As $N'$ increases, the branching ratios gradually become similar to

those resulting from the single state dissociation via the $^2\Sigma^-$ state, indicating that the dissociation is mainly by the coupling between the $A^2\Sigma^+$ and the $^2\Sigma^-$ states for higher $N'$. This change in the branching ratios with respect to $N'$ can easily be expected by considering the positions of the resonances in Figure 1: The lower resonance with $N' = 0$ lies between the crossing points of the $A^2\Sigma^+$ state with the two repulsive $^2\Sigma^-$ and $^4\Sigma^-$ states, while those with higher $N'$ get closer to the crossing point of the $A^2\Sigma^+$ and the $^2\Sigma^-$ states.

## Conclusions

We have systematically investigated the branching ratios and the vector properties of the triplet oxygen atom produced from the photodissociation of the OH molecule near the $v' = 4$ resonances of the $A^2\Sigma^+$ state. We find that the total and partial cross sections are essentially Lorentzian, indicating that the effects of quantum interference are minimal. On the other hand, the influence of the multichannel asymptotic interactions could clearly seen by the effects on the vector properties near the isolated resonances as monotonous but noticeable changes of the vector properties. For overlapping $F_1$ and $F_2$ resonances, the abrupt changes in the fragments vector properties exhibit the effects of overlapping, which cannot be seen in the scalar properties. Experimental studies on these findings will be highly desirable.

**Acknowledgment**. This work was supported by the Korea Science and Engineering Foundation (1999-1-121-001-5).

## References

1. Singer, S. J.; Freed, K. F.; Band, Y. B. *Adv. Chem. Phys.* **1985**, *61*, 1; *J. Chem. Phys.* **1983**, *79*, 6060.
2. (a) Williams, C. J.; Freed, K. F.; Singer, S. J.; Band, Y. B. *Faraday Discuss. Chem. Soc. 2* **1986**, *82*, 1. (b) Williams, C. J.; Freed, K. F. *J. Chem. Phys.* **1986**, *85*, 2699.
3. Strube, W.; Singer, S. J.; Freed, K. F. *Chem. Phys. Lett.* **1984**, *110*, 588.
4. Singer, S. J.; Freed, K. F.; Band, Y. B. *Chem. Phys. Lett.* **1982**, 91, 12; *J. Chem. Phys.* **1985**, *81*, 3091.
5. Alexander, M.; Pouilly, B.; Duhoo, T. *J. Chem. Phys.* **1993**, *99*, 1752.
6. Lee, S.; Jung, K.-H. *J. Chem. Phys.* **2000**, *112*, 2810.
7. Zhang, J.; Dulligan, M.; Wittig, C. *J. Chem. Phys.* **1997**, *107*, 1403.
8. Regan, P. M.; Langford, S. R.; Orr-Ewing, A. J.; Ashfold, M. N. R. *J. Chem. Phys.* **1999**, *110*, 281.
9. Peoux, G.; Monnerville, M.; Duhoo, T.; Pouilly, B. *J. Chem. Phys.* **1997**, *107*, 70.
10. Lee, S. *J. Chem. Phys.* **1995**, *103*, 3501.
11. Lee, S. *Bull. Korean. Chem. Soc.* **1995**, *16*, 387; *Chem. Phys. Lett*. **1995**, *240*, 595; *Bull. Korean. Chem. Soc.* **1995**, *16*, 801; *J. Chem. Phys.* **1996**, *104*, 1912; *Chem. Phys. Lett.* **1995**, *243*, 250; *J. Chem. Phys.* **1996**, *104*, 7914; *J. Chem. Phys.* **1997**, *107*, 1388.
12. Lee, S. *Phys. Rev.* A **1998**, *58*, 4981.
13. Lee, S. *J. Chem. Phys.* **1999**, *111*, 6407.
14. Gray, J. A.; Farrow, R. L. *J. Chem. Phys.* **1991**, *95*, 7054.
15. Heard, D. E.; Crosley, D. R.; Jeffries, J. B.; Smith, G. P.; Hirano, A. *J. Chem. Phys.* **1992**, *96*, 4366.
16. Brzozowski, T.; Erman, P.; Lyyra, M. *Phys. Scr.* **1978**, *17*, 507.
17. Lee, S. *Bull. Korean Chem. Soc.* **1995**, *16*, 449.
18. Yarkony, D. R. *J. Chem. Phys.* **1992**, *97*, 1838.
19. Sink, M. L.; Bandrauk, A. *J. Chem. Phys.* **1980**, *73*, 4451; *Chem. Phys. Lett.* **1979**, *65*, 246.
20. Parlant, G.; Yarkony, D. R. *J. Chem. Phys.* **1999**, *110*, 363.
21. (a) Lee, S.; Wlliams, C. J.; Freed, K. F. *Chem. Phys. Lett.* **1986**, *130*, 271. (b) Lee, S.; Freed, K. F. *J. Chem. Phys*. **1987**, *87*, 5772.
22. Cooley, J. W. *Math. Comp.* **1961**, *383*, 15.
23. Johnson, B. R. *J. Chem. Phys.* **1977**, *67*, 4086.
24. Greene, C. H.; Zare, R. N. *Annu. Rev. Phys. Chem.* **1982**, *33*, 119; *J. Chem. Phys.* **1983**, *78*, 6741.
25. Fano, U.; Macek, J. H. *Rev. Mod. Phys.* **1973**, *85*, 553.
26. (a) Dubs, R. L.; Julienne, P. S. *J. Chem. Phys.* **1991**, *95*, 4177. (b) Dubs, R. L.; Julienne, P. S.; Mies, F. *J. Chem. Phys.* **1990**, *93*, 8784.
27. Wang, J. X.; Kleiber, P. D.; Sando, K. M.; Stwalley, W. C. *Phys. Rev. A* **1990**, *42*, 5352.
28. Zhang, J.; Riehn, C. W.; Dulligan, M.; Wittig, C. *J. Chem. Phys.* **1996**, *104*, 7027.
29. Kim, Y. S.; Jung, Y.-J.; Jung, K.-H. *J. Chem. Phys.* **1997**, *107*, 3805.
30. Liyanage, R.; Yang, Y.-A.; Hashimoto, S.; Gordon, R. J.; Field, R. W. *J. Chem. Phys.* **1995**, *103*, 6811.